Conflict assessment and resolution of climate-optimal aircraft trajectories at network scale

Fateme Baneshi [*], Manuel Soler, Abolfazl Simorgh

Department of Aerospace Engineering, Universidad Carlos III de Madrid, Avenida de la Universidad, 30, Leganes, 28911 Madrid, Spain

A R T I C L E   I N F O

A B S T R A C T

Aviation contributes to anthropogenic climate change through carbon dioxide (CO_2) and non-CO_2 emissions. Due to dependency on atmospheric conditions, the non-CO_2 climate impacts can be mitigated using aircraft trajectory optimization. However, adopting independently optimized trajectories may not be operationally feasible for the air traffic management system due to the associated impacts on the safety, demand, and complexity of air traffic. This study aims to explore the effects of employing climate-optimized trajectories on air traffic complexity in terms of the number of conflicts and propose a strategic resolution based on speed change to resolve the conflicts that arise. A scenario with 1005 flights is considered as the case study. The results indicate that the adoption of climate-optimal trajectories increases operational cost and the number of conflicts. Employing the proposed resolution algorithm, it is shown that the conflicts can be resolved by accepting slight increases in climate impact and cost.

1. Introduction

The aviation sector's contribution to global warming requires the consideration of both carbon dioxide (CO_2) and non-CO_2 emissions. The agents of non-CO_2 emissions that contribute to global warming include nitrogen oxides (NO_x), sulfur oxides (SO_x), carbon monoxide(CO), unburnt hydrocarbons (HC), particulate matter (PM), soot, water vapor (H_2O), and persistent contrail and contrail-cirrus formations (Lee et al., 2021). The climate impact of non-CO_2 emissions, though still needs further scientific understanding, has been claimed to potentially be two times higher than CO_2, in which the highest contribution corresponds to contrails in terms of radiative forcing (Lee et al., 2021). The effects of non-CO_2 species on climate depend directly on the geographical location, altitude, and time of the emissions (Lee et al., 2021). Consequently, their impact can be potentially mitigated with operational strategies, especially aircraft trajectory optimization (Matthes et al., 2020). Interested readers are referred to Simorgh et al. (2022) for a recent, comprehensive survey on climate-optimal aircraft trajectory planning.

Mitigation of non-CO_2 climate impact in the aviation context requires, to start with, information on sensitive regions to climate impact. Within the EU-project ATM4E, algorithmic climate change functions (aCCFs) were developed to identify such areas. The aCCFs take atmospheric variables, including geopotential, potential vorticity, and outgoing longwave radiation, from standard weather forecasts and quantify the climate impact caused by each species in terms of average temperature response (ATR) (Matthes et al., 2020). The analysis of the potentiality to mitigate the climate effects of non-CO_2 emissions employing aCCFs has been investigated in several studies (see Simorgh et al. 2022 and references therein).

Despite the numerous studies devoted to the exploration of climate impact mitigation potential at the micro-scale (trajectory level), the consideration of climatic impact at the network scale is still lacking and has been identified as a scientific gap (Simorgh

---

et al., 2022). Indeed, the ATM network system is a multi-agent system that cannot be characterized by individual elements but by their collective behavior at the network scale. Therefore, considering climate impact at the trajectory scale without analyzing its effects at the network scale does not reflect real operational scenarios. To this end, a climate-oriented ATM system should necessarily consider network effects such as, just to mention a few, safety, complexity, resiliency, and capacity-demand balancing. For instance, adopting independently optimized aircraft trajectories to mitigate the climate impact may result in more congested airspace around climate-sensitive areas, raising some challenges, particularly the increase in workload, complexity, and the number of conflicts. Consequently, this would result in capacity-demand imbalances. In this respect, the assessment of how the climate-optimal trajectories affect the ATM system requires network-related indicators. So far, many indicators have been proposed in the literature to describe different aspects of the ATM performance, including workload (Socha et al., 2020), complexity (Prandini et al., 2011), and resiliency (Jakšić and Janić, 2020). Among all the mentioned indicators, in this paper, we focus on complexity. Though there is not a universal agreement on the complexity definition, it can be defined as a measure of difficulty and required effort to manage air traffic in an efficient and safe manner. Many metrics have been reported in the literature to evaluate complexity, such as adjusted density (Pejovic et al., 2020), traffic density (Hilburn, 2004), and the number of conflict (Allignol et al., 2017). In this respect, Hilburn (2004) conducted a review in which up to 100 different complexity indicators were reported to model traffic complexity either individually or with linear or non-linear combinations.

Besides the potential negative effects of adopting climate-optimal trajectories on air traffic performance, rerouting sensitive areas to climate increases the operating costs compared to the "Business-as-Usual" (BAU) trajectories as the aircraft tends to fly longer routes. In this respect, two main incentives are generally required for airliners to adopt climate-optimal routes: (1) manageability of air traffic in a safe and operationally feasible manner, and (2) acceptability of operating costs. The focus of our study is aligned with the first motivation, i.e., manageability of the adverse effects of considering climate-optimal trajectories on the ATM system's performance. However, regarding incentives associated with the operating cost, there is a need for climate policy (Niklaß et al., 2019). Although the emission of CO_2 is included in some market-based instruments such as emission trading schemes (ETS), it is still lacking for non-CO_2 emissions. Several studies have been proposed in the literature aiming at setting up market-based instruments for aviation non-CO_2 climate effects (see e.g., Niklaß et al. 2021 for the concept of climate-charged airspace). If taxes are considered for emitting in highly sensitive regions to the aviation-induced non-CO_2 climate effects, the climate-optimal trajectories will be economically beneficial.

Given a set of climatically-optimal trajectories, one can summarize the open problems as follows: (1) assessment of the fostered effects of considering climate impact at the network scale, (2) proposing resolution strategies to compensate for the arisen negative impacts due to the consideration of climate impact. In light of the challenges described above, as a preliminary step, we aim to investigate the effects of adopting climate-optimized trajectories on traffic patterns and then propose a resolution strategy to counteract the adverse consequences. The number of conflicts as an important indicator of complexity and safety is considered and included in the objective function to be minimized with respect to minimum deviation from climate-optimal trajectories.

In literature, though not related to the consideration of climate impact, one can find different selection of decision variables and objectives to solve the resolution problem at network scale with various solution approaches including meta-heuristic (Courchelle et al., 2019), learning-based (Tran et al., 2019), mathematical programming (Pelegrín and d'Ambrosio, 2022), and gradient-based methods (Hernández Romero, 2020). In this paper, simulated annealing is employed as the solution approach to resolving the conflicts, considering the speed profiles as decision variables. The problem of resolving arisen challenges associated with employing climate-optimal trajectories can be stated as an optimization problem to generate new sets of trajectories with respect to the following two objectives: (1) adherence of modified trajectories to the climate-optimal ones as an indicator of climate efficiency, (2) resolution of the arisen negative impacts due to the consideration of climate impact (e.g., complexity, conflict, and workload). The decision variables in this optimization problem can be the speed profile, lateral path, altitude, departure time, and a combination of them.

To consider a network-scale traffic scenario, we use the information of the Eurocontrol's Demand data repository (DDR2) dataset[1] (e.g., origin, destination, time, cruise altitude) and limit the dataset to the flights in an area of airspace mainly covering Spain and Portugal for four hours, yielding 1005 flights. We employ the aCCFs reported in Yamashita et al. (2020) for quantifying the climate impacts of CO_2 emission and different non-CO_2 species. The predicted climate impact quantified using aCCFs and aircraft trajectories are affected by uncertainties in atmospheric variables. Due to the propagation of uncertainties at the network scale, ignoring such possible deviations in the estimated aircraft performance and climate impact can result in unreliable mitigation potential and inaccurate conflict assessment. To have a quantification of uncertainty, we make use of the ensemble prediction system (EPS), providing N_{EPS} probable realizations of weather variables (WMO, 2012). The trajectory optimization is performed by taking the mean values of ensemble members for each flight using the direct optimal control approach, considering different user-defined routing options ranging from cost to climate-optimal ones. Then, the ensemble trajectory prediction is proposed to reflect the uncertainty associated with the weather forecast on the optimized trajectories. The effects caused by considered routing options are assessed in terms of the number of conflicts by employing a grid-based conflict detection algorithm. Due to variability in the components of wind within the EPS weather forecast, there exist some degrees of uncertainty in the time aircraft fly the determined trajectories. To this end, the conflict assessment is performed in a probabilistic manner. It is shown for the considered scenario that by moving toward trajectories with lower climate impacts, the number of conflicts increases due to the congestion around climate-sensitive areas. As changes in the traffic patterns due to adopting climate-optimal trajectories increase the number of conflicts that may not be manageable at the tactical level, resolution strategies are required to improve the safety level of the
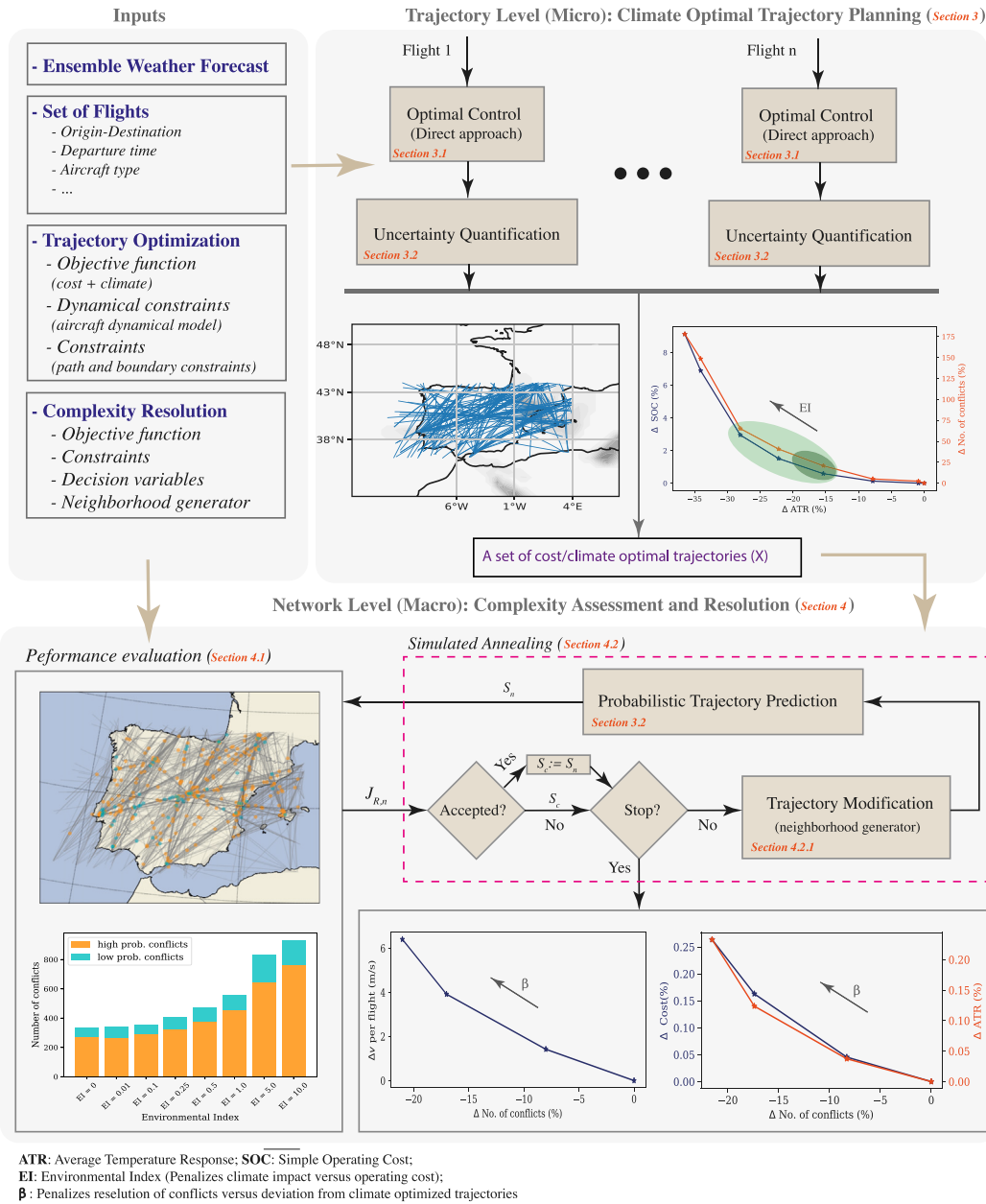
---

[1] https://www.eurocontrol.int/ddr

Fig. 1. Overview of the methodology.

airspace by strategically resolving the encountered conflicts. The resolution algorithm should generate new maneuvers that are safe, in terms of reducing the number of conflicts, and efficient such that the new trajectories remain as close as possible to the climate-optimal ones. As this problem is a large-scale optimization problem including many decision variables, we rely on SA as the solution approach. To avoid blindly decisions making, we inform the SA algorithm by defining an efficient neighborhood generator function.

The structure of the paper is organized as follows. The problem statement and modeling are presented in Section 2. The approach to optimize micro-scale trajectories is stated in Section 3, and Section 4.1 presents the technique employed for calculating the number of conflicts. In Section 4.2, a deconfliction algorithm is proposed for the resolution process. The simulation results considering 1005 flights are provided in Section 5. Section 6 closes the paper by presenting some concluding remarks and our planned works for the future.

2. Problem statement and modeling

In this study, our goal is to determine network-wide climate-optimized trajectories within two layers shown in Fig. 1. In the first layer, we optimize each trajectory independently in a climate-friendly manner. The performance of the determined climate-optimal trajectories in terms of the number of conflicts is assessed in the second layer, and a resolution strategy to resolve the encountered conflicts is performed within an optimization framework. In this respect, we briefly present the items needed to formulate trajectory optimization, conflict detection, and conflict resolution problems. These elements are the aircraft dynamical model, climate impacts associated with aircraft emissions, and uncertainty quantification.

2.1. Aircraft dynamical model

To optimize and predict the motion of aircraft, we use the point-mass model, where the aerodynamics and performance of aircraft are given by the BADA model (BADA 4 in this study Gallo et al., 2006) (González-Arribas et al., 2017):

$$
\begin{aligned}
\frac{d\varphi}{dt} &= \frac{(v\cos\chi + w_x)}{R_N + h} \\
\frac{d\lambda}{dt} &= \frac{v\sin\chi + w_y}{(R_M + h)\cos\varphi} \\
\frac{dv}{dt} &= \frac{1}{m}\left(T(C_T) - D(m,v)\right) \\
\frac{dm}{dt} &= -f_c(C_T).
\end{aligned}
\tag{1}
$$

In Eq. (1), φ is the latitude, λ is the longitude, h is the altitude, m is mass, R_M and R_N represent the radii of curvature of ellipsoid and meridian and prime vertical, respectively, f_c is the rate of fuel burn, T is the magnitude of thrust force, D is the magnitude of drag force, C_T is the thrust coefficient, v is the true speed, (w_x, w_y) are the wind components, and χ is the heading angle. In this representation, the state and control vectors are defined as

$$
\begin{aligned}
\mathbf{x} &= \begin{bmatrix} \varphi & \lambda & v & m \end{bmatrix}, \\
\mathbf{u} &= \begin{bmatrix} \chi & C_T \end{bmatrix}.
\end{aligned}
\tag{2}
$$

2.2. Climate impact

To include the climate impact associated with aircraft emissions in the trajectory planning, the algorithmic climate change functions (aCCFs) reported in Yamashita et al. (2020) are adopted. These functions, developed during the EU-project ATM4E, take the meteorological variables as input and quantify the climate impacts due to the emissions of CO_2, NO_x and water vapor, and the formation of persistent contrails in terms of average temperature response (ATR) over a period of 20 years (ATR20). The interested readers are referred to Yamashita et al. (2020), van Manen and Grewe (2019) for the detailed description of these functions.

2.3. Uncertainty

The climate impact of non-CO_2 emissions highly relies on meteorological conditions, including temperature, relative humidity, and outgoing longwave radiation (Matthes et al., 2020; Yamashita et al., 2020). Therefore, a factor that can affect the reliability of the quantified climate impacts is the quality of the weather forecast (Matthes et al., 2017). The weather forecast is inevitably uncertain (Bauer et al., 2015), which can also affect the aircraft trajectories due to dependency on wind and temperature (González Arribas et al., 2020). Ensemble prediction systems (EPS) have been introduced to quantify the uncertainties associated with the weather forecast, providing a collection of N_{EPS} different realizations of weather situations called ensemble members. Forecasts within EPS can be obtained using different techniques. For instance, in one approach called ensemble data assimilation, the initial conditions or/and parameters of models used in producing forecasts are perturbed.

3. Climate-optimized trajectories

The proposed aircraft trajectory planning approach for considering climate impact is presented in two steps: trajectory optimization and, then, trajectory prediction considering atmospheric uncertainty (to quantify the associated uncertainty in the aircraft trajectory and its climate impact).

3.1. Trajectory optimization

In the optimization step we take the mean values of the ensemble weather variables and solve the trajectory optimization problem in a deterministic manner using the aircraft dynamical model given in Section 2.1 with the following objective function and boundary and path constraints:

1. Objective function:

$$J = \text{CI} \underbrace{\left[\text{C}_t \cdot \left[t_f - t_0 \right] + \text{C}_f \cdot \left[m(t_0) - m(t_f) \right] \right]}_{\text{SOC}} + \text{C} \cdot \text{EI} \underbrace{\int_{t_0}^{t_f} \sum_{i=1}^{5} \text{ATR}_i^{\text{mean}} \left(t, \mathbf{x}(t), \mathbf{u}(t) \right) \mathrm{d}t}_{\text{ATR}}, \tag{3}$$

for $i \in \{\text{CH}_4, \text{Contrails}, \text{O}_3, \text{H}_2\text{O}, \text{CO}_2\}$, where $\mathbf{x}(t)$ and $\mathbf{u}(t)$ are the state and control vectors, respectively, and SOC is the simple operating cost (Yamashita et al., 2020). $\text{ATR}_i^{\text{mean}}$ is the ATR for the agent i calculated from considering mean values of ensemble members. The ATR for different non-CO_2 species are calculated as follows:

$$\begin{aligned}
\text{ATR}_{\text{O}_3}(t, \mathbf{x}, \mathbf{u}) &= 10^{-3} \times \text{aCCF}_{\text{O}_3}(t, \mathbf{x}) \cdot \text{EI}_{\text{NO}_x}(t, \mathbf{x}, \mathbf{u}) \cdot f_c(\mathbf{u}) \\
\text{ATR}_{\text{CH}_4}(t, \mathbf{x}, \mathbf{u}) &= 10^{-3} \times \text{aCCF}_{\text{CH}_4}(t, \mathbf{x}) \cdot \text{EI}_{\text{NO}_x}(t, \mathbf{x}, \mathbf{u}) \cdot f_c(\mathbf{u}) \\
\text{ATR}_{\text{Contrails}}(t, \mathbf{x}) &= 10^{-3} \times \text{aCCF}_{\text{Contrails}}(t, \mathbf{x}) \cdot v_{gs}(t) \\
\text{ATR}_{\text{H}_2\text{O}}(t, \mathbf{x}, \mathbf{u}) &= \text{aCCF}_{\text{H}_2\text{O}}(t, \mathbf{x}) \cdot f_c(\mathbf{u})
\end{aligned} \tag{4}$$

where v_{gs} is the ground speed and $\text{EI}_{\text{NO}x}(t, \mathbf{x}, \mathbf{u})$ is the NO_x emission index calculated using Boeing Fuel Flow Method 2 (DuBois and Paynter, 2006). To explain how the $\text{ATR}_i^{\text{mean}}$ for the agent i is calculated, let us consider aCCF of water vapor. According to Yamashita et al. (2020), aCCF of water vapor depends on the meteorological variable potential vorticity. Since within EPS, we are provided with N_{EPS} forecasts, N_{EPS} different aCCFs can be calculated for water vapor. Thus, $\text{ATR}_{\text{H}_2\text{O}}^{\text{mean}}(\cdot)$ indicates that the ATR is calculated from considering the average of aCCFs obtained from different ensemble members. As can be seen, the defined objective function considers both climate impact and cost. Normally, there exists a trade-off between these two objectives. Weighting parameters environmental index (EI) and cost index (CI) determine the importance of these objectives compared to each other. Moreover, constant parameters C_t and C_f are used for allowing different explanations of cost, and C adjusts the order of climate impact with cost.

2. Path constraints:

$$\begin{aligned}
v_{CAS,stall} &\leq v_{CAS}(v) \leq v_{CAS,\max} \\
C_{T,\min} &\leq C_T \leq C_{T,\max} \\
M(v_{tas}) &\leq M_{\max}
\end{aligned} \tag{5}$$

where M is the Mach number and v_{CAS}, is the calibrated airspeed.

3. Boundary constraints:

$$\begin{aligned}
\left[\varphi, \lambda, v \right](0) &= \left[\varphi_0, \lambda_0, v_0 \right] \\
\left[\varphi, \lambda, v \right](t_f) &= \left[\varphi_f, \lambda_f, v_f \right] \\
m(0) &= m_0.
\end{aligned} \tag{6}$$

The direct optimal control approach as an efficient technique for solving highly nonlinear dynamical optimization problems with different sets of constraints is employed to solve the formulated trajectory optimization problem (Simorgh et al., 2022). In this approach, the dynamical optimization problem (trajectory optimization problem in our case) with the objective function, dynamical model, and different types of constraints (e.g., path and boundary constraints) is transcribed to a nonlinear programming problem (NLP) represented with the following general form (Betts, 2010):

$$\min_{\Theta} \quad J_{NLP}(\Theta) \tag{7}$$

$$\text{s.t} \quad \Phi_i(\Pi) = 0 \quad i = 1, \ldots, n_\omega \tag{8}$$

$$\Xi_i(\Theta) \leq 0 \quad i = 1, \ldots, n_\xi \tag{9}$$

where the vector $\Theta \in \mathbb{R}^{n_\Theta}$ includes the decision (or NLP) variables, and equality and inequality constraints are represented by Eqs. (8) and (9), respectively. The optimal solution to the original dynamical optimization problem is obtained by solving the resulting discretized problem. The NLP problems can be solved using various techniques, such as gradient-based and meta-heuristic methods. Moreover, several efficient software packages, including IPOPT (Biegler and Zavala, 2009) and SNOPT (Andrei, 2017), exist for solving such a class of optimization problems. Interested readers are referred to Betts (2010) for more details on the direct optimal control approach.

After solving the trajectory optimization problem, an optimal trajectory for the aircraft ith is received and denoted as $T_i^o :=$ $(\varphi_i^o, \lambda_i^o, v_i^o)$.

3.2. Ensemble trajectory prediction

In the prediction step, we evaluate the performance of the optimized trajectory $T_i^o := (\varphi_i^o, \lambda_i^o, \upsilon_i^o)$ for all ensemble members. First of all, we assume a unique lateral path and speed profile (obtained from trajectory optimization) for all ensemble members. The consideration of a unique lateral path implies a constant aircraft course (ψ^o). In this case, the uncertainty will affect ground speed as:

$$\upsilon_{gs}^m = \sqrt{\upsilon^2 + w_c^{m^2}} + w_a^m, \tag{10}$$

where (w_a, w_c) is the decomposition of wind along the along-track and cross-track directions and $(\cdot)^m$ denotes the ensemble member m. The uncertainty in ground speed affects the time aircraft flies the trajectory through

$$\frac{\mathrm{d}t^m}{\mathrm{d}s} = (\upsilon_{gs}^m)^{-1}, \tag{11}$$

where t^m is the flight time associated with the ensemble member m and s is the distance flown along route. The fuel consumption is also predicted in a similar way. Now, we consider the range of uncertainty in the climate impact. For the ensemble member m, one has

$$\mathrm{ATR}^m = \int_{t_0^m}^{t_f^m} \sum_{i=1}^{5} \mathrm{ATR}_i^m\big(t^m, \mathbf{x}^m(t^m), \mathbf{u}(t^m)\big)\mathrm{d}t^m, \tag{12}$$

where the superscript m in $\mathbf{x}^m$ is due to the calculated ensemble values for aircraft mass within ensemble trajectory prediction. As can be concluded, the uncertainty due to the weather forecast has been reflected in flight time, fuel consumption, and climate impacts, resulting N_{EPS} different values at each integration step. Different moments of the ensemble distribution can be performed on these values, such as average and standard deviation. The proposed approach provides valuable insight into the impacts of uncertainty associated with weather forecasts on aircraft trajectories. For the unique profile determined in the optimization step, the effects of uncertainty are quantified and reflected on the flight time, fuel consumption, and climate impacts which are included in:

$$\Gamma_i := \{(t_i^1, \dots, t_i^{N_{EPS}}), (m_i^1, \dots, m_i^{N_{EPS}}), (\upsilon_{gs_i}^1, \dots, \upsilon_{gs_i}^{N_{EPS}}), (\mathrm{ATR}_i^1, \dots \mathrm{ATR}_i^{N_{EPS}})\}. \tag{13}$$

4. Conflict assessment and resolution

The adoption of independently determined climate-optimal trajectories can result in more congested areas due to the avoidance of climate-sensitive regions, leading to safety issues, capacity-demand imbalance, and increased complexity and workload within the ATM system. In this respect, a preliminary step toward finding operationally feasible trajectories within the network scale is to assess the arisen challenges and then implement resolution strategies to compensate for the adverse effects.

In this study, the impact of employing climate-optimal trajectories at the network scale is assessed in terms of the number of conflicts (presented in Section 4.1). Then, a resolution strategy is proposed to solve the encountered conflicts (Section 4.2).

4.1. Probabilistic conflict detection

A conflict is defined as an event in which an aircraft loses its standard separation from other aircraft or airspace constraints, leading to safety degradation. One criterion of standard separation is $D_0 = 5$ NM of horizontal distance and $H_0 = 1000$ ft vertical distance. In other words, a cylinder with a 5 NM diameter and 1000 ft height can represent a protected zone for each aircraft that should not be intersected with other aircraft-protected zones. The aim of conflict detection is to predict probable loss of separation that may occur in the future at a specific time and position. Conflict detection for large-scale scenarios generally suffers from computational time since most algorithms compute conflicts pairwise. Moreover, the inputted trajectories for conflict detection may have some perturbations due to the consideration of uncertainty, such as the ones proposed in Section 3. To deal with the mentioned concerns (i.e., computational time and uncertainty), we employ the probabilistic grid-based technique firstly proposed in Hernández Romero (2020). Within this technique, aircraft trajectories are saved into grids cells (the size of each cell should be greater or equal to the minimum standard separation) as depicted in Fig. 2 (Hernández Romero, 2020). One challenge associated with the implementation of this method is the required memory to store all grids. To deal with this issue, the hash table structure is employed (Hastings et al., 2005). The hash table extensively reduces the required memory as we neglect empty cells. The conflict between aircraft k and l is evaluated if their assigned cells are the same or are neighboring. In this case, their distance corresponding to the ensemble member m is computed at the time instant Δt_n. If the computed distance is less than the standard separation, there exists a conflict, i.e.,

$$p_{kl}^m = \begin{cases} 1 & \text{if} \quad d_{kl}^m < D_0 \quad \text{and} \quad h_{kl}^m < H_0 \\ 0 & \text{else} \end{cases} \tag{14}$$

where d_{kl} and h_{kl} are the horizontal and vertical distances, respectively. The probability of conflict between aircraft k and aircraft l is then calculated over all ensemble members as:

$$\mathrm{P}_{c,kl} = \frac{1}{N_{EPS}} \sum_{m=0}^{N_{EPS}} p_{kl}^m \tag{15}$$

where N_{EPS} represents the number of ensemble members.
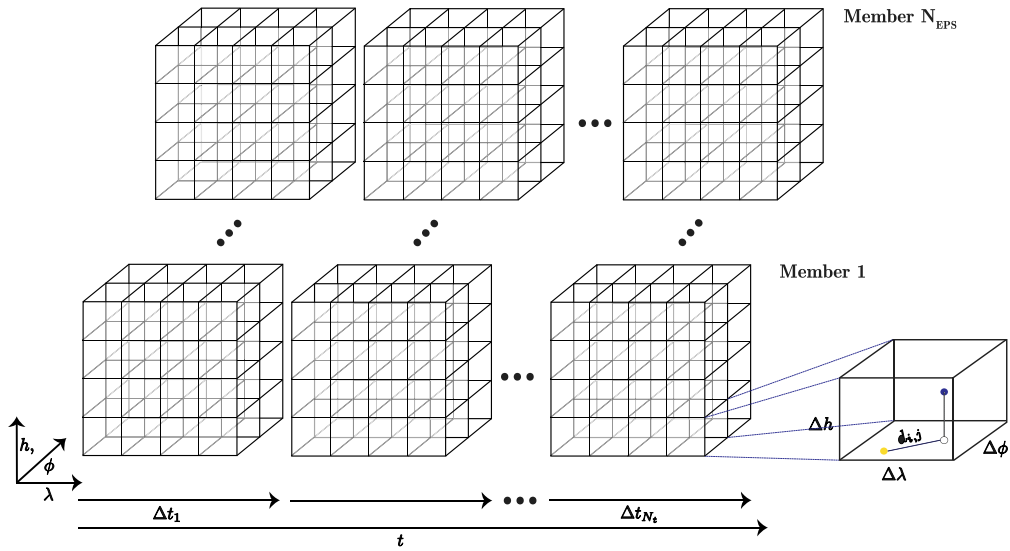
Fig. 2. Grid-based representation of space duplicated with the number of ensemble members.

4.2. Conflict resolution

In resolution strategies, aircraft trajectories are modified to generate new maneuvers that are safe in terms of reducing the number of conflicts and efficient such that the new trajectories remain as close as possible to the inputted trajectories. In this study, the resolution procedure is stated as a nonlinear programming problem with the following two objectives, subject to some constraints.

- Minimum deviation of the modified trajectories from the climate-optimal ones.
- Minimum number of high probable conflicts.

These objectives are mathematically modeled and included in the following cost function

$$J_R = \beta.K.\Sigma + (1 - \beta) \sum_{i=1}^{N} (\Delta v_i) \tag{16}$$

where N represents the number of flights. $\beta \in [0,1]$ is a weighing parameter that determines the importance of the mentioned objectives compared to each other, K is the scaling parameter, and Σ is the number of high probable conflicts defined as

$$\Sigma = 0.5 \sum_{k=1, k \neq l}^{N} \sum_{l=1}^{N} Y_{kl}, \qquad Y_{kl} = \begin{cases} 1 & \text{if} \quad P_{c,kl} \geq P_\tau \\ 0 & \text{else} \end{cases} \tag{17}$$

where the parameter P_τ is a user-defined probability threshold that allows users to adjust the level of conservativeness. For instance, $P_\tau = 0$ considers all possible conflicts caused by ensemble members (both high and low probability conflicts) to be resolved while $P_\tau \geq 0.5$ only considers those conflicts that occur at least within half of the ensemble members.

The decision variables of the optimization problem are the true airspeed of each flight. The speed change (deviation from climate-optimal speed) is constrained as:

$$-0.06 \leq \Delta v \leq 0.04. \tag{18}$$

Due to the complexity of the optimization problem (i.e., a large number of decision variables), we rely on the SA algorithm as the solution approach (Courchelle et al., 2019). The SA algorithm inspired by the annealing process aims at reaching the minimum energy of metal by rearranging its particles. This algorithm is based on temperature change through the heating and cooling process. In the heating process, the particles have enough freedom to move around in random directions. By reducing the temperature, they tend to find a new stable configuration to achieve minimum energy (Dowsland and Thompson, 2012). The SA in optimization applications uses the same strategy to minimize a defined objective function. A neighbor solution is generated at each iteration, and its associated cost is compared with the current solution. The generated solution at each iteration is accepted with a probability that is related to the temperature and difference between the current and new costs. At the beginning of the process, where the temperature is high, the worse solutions (i.e., the solutions that yield higher costs compared to the previous step) are more likely to be accepted. The acceptance rate of the worse solutions is reduced within the cooling process. The property to accept worse solutions provides the ability to avoid getting stuck in local minima and is one of the main advantages of SA over the gradient-based solvers such as interior-point, and successive quadratic programming (Dowsland and Thompson, 2012).

For the considered resolution problem, at each iteration, a neighbor solution is generated from the neighborhood function (presented in Section 4.2.1) and the objective function Eq. (16) is re-evaluated ($J_{R,n}$). The new cost $J_{R,n}$ is compared with the current cost $J_{R,c}$ and accepted with the following probability

$$P_{acc} = \begin{cases} 1 & \text{if} \quad J_{R,n} \leq J_{R,c} \\ e^{-(J_{R,n}-J_{R,c})T^{-1}} & \text{else.} \end{cases} \tag{19}$$

According to Eq. (19) if the cost associated with the neighbor solution is improved, it is accepted, and in the case of degradation, it is accepted with the defined probability (obtained from Boltzmann distribution).

4.2.1. Neighborhood function

At each iteration within SA, new solutions need to be generated, called neighbor solutions. Here, we propose a neighborhood function to generate candidate solutions by modifying the aircraft's true airspeed. To avoid blindly exploring within a large search space, we inform the algorithm only to modify the trajectories of aircraft in conflict. The proposed algorithm starts from a set of climate-optimal trajectories (determined in Section 3.1) as initial solution S_0 with the cost $J_{R,0}$. At each iteration, the neighborhood function generates a neighbor solution S_n with the cost $J_{R,n}$. The steps to generate a neighbor solution within the neighborhood function are as follows:

1. two sets of aircraft, including 20 aircraft with more conflicts Ω_1 and 20 aircraft with more deviation from optimal speed Ω_2, are selected separately,
2. an aircraft to be modified Ac_m is selected with the probability β from the set Ω_1, and $1 - \beta$ from the set Ω_2. By this setting, with increasing β, the aircraft with higher number of conflicts are more likely to be selected for the resolution,
3. the airspeed v_m of Ac_m is modified within the defined permissible range, and its associated performance Γ_m is re-computed employing the ensemble trajectory prediction method presented in Section 3.2.

The SA algorithm and the proposed neighborhood function are presented in Algorithm 1.

Algorithm 1 SA Algorithm

Require: $N_{tr}, \alpha, T_{in}, T_f, \beta$
Require: A set of climate-optimal trajectories S_0
  $T_c \leftarrow T_{in}$, $J_{R,c} \leftarrow J_{R,0}$, $S_c \leftarrow S_0$
  while $T_c < T_f$ **do**
      $N_c \leftarrow 0$
      while $N_c < N_{tr}$ **do**
          From Sc get subsets Ω_1 and Ω_2.
          Get a random number $p \in [0, 1]$
          if $p \leq \beta$ **then**
              Get random aircraft $Ac_m \in \Omega_1$
          else
              Get random aircraft $Ac_m \in \Omega_2$
          end if
          Get random number $\gamma \in [0.96, 1.04]$
          $v_m^o \times \gamma$
          Predict the aircraft performance Γ_m
          Compute $J_{R,n}$
          if $J_{R,n} \leq J_{R,c}$ **then**
              Replace the new profile of Ac_m in S_c
              $J_{R,c} \leftarrow J_{R,n}$
          else
              Get a random number $\sigma \in [0, 1]$
              $P_{acc} \leftarrow e^{-(J_{R,n}-J_{R,c})T^{-1}}$
              if $\sigma < P_{acc}$ **then**
                  Replace the new profile of Ac_m in S_c
                  $J_{R,c} \leftarrow J_{R,n}$
              end if
          end if
          $N_c \leftarrow N_c + 1$
      end while
      $T_c \leftarrow T_c \times \alpha$
  end while
  $S^* \leftarrow S_c$
  Return S^*

---

5. Simulation results

A case study including 1006 flights is presented to illustrate the applicability of the proposed methodology. In Section 5.1, the independently optimized trajectories are determined for different routing options. The effects of considering the optimized trajectories at the network scale are assessed in terms of the number of conflicts in Section 5.2, which is then resolved in Section 5.3.

5.1. Trajectory optimization

The flight data have been extracted from the DDR2 dataset by limiting airspace to an area mainly covering Spain and Portugal on May 6th 2018 from 12:00 to 16:00. The information regarding the origin, destination, cruise altitude, and flight time have been provided within the DDR2 dataset. The aircraft models are all considered to be A330-341 with an initial mass of 200 tons. To model the uncertainty in meteorological variables, the ERA5 data products[2] containing ten ensemble members is adopted and used in trajectory optimization and prediction steps. It is worth mentioning that the reanalysis data are not suitable for flight planning since they are generated from post-processing with observations. Due to ease of availability, we employ this dataset in this study, however, forecast data with different number of ensemble members can be employed in a similar manner. The extracted flights are optimized with the direct optimal control approach for the problem formulated in Section 3.1 considering the mean values of ensemble members for weather variables. We use the Trapezoidal rule to transcribe the original optimal control problem to the nonlinear programming problem. The resulting NLP problem is then solved using the IPOPT solver in Python, employing the interior-point method to find the optimal solution. The number of discretization nodes is N_d=100. The discretized shortest path is considered as the initial guess for the optimizer. The trajectories are optimized in 2D airspace for eight different environmental indices (i.e., EI [-]), considering CI = 1.0 [-], C_t = 0.75 [USD/s], C_f = 0.51 [USD/kg] and C = 10^{14} [USD/K]. To quantify the uncertainty on the flight performances due to the ensemble members, the ensemble trajectory prediction proposed in Section 3.2 is implemented. For each weighting coefficient, the computational time to solve the trajectory optimization and prediction for all flights are approximately 100 min (i.e., 6s per flight) of CPU time. The optimized trajectories for two environmental indices are depicted in Fig. 3. According to the recent studies employing aCCFs to quantify climate impact (Yamashita et al., 2020, 2021), the climate effect of contrails outweighs the impacts caused by other species. To this end, the optimized trajectories are plotted with the aCCF of contrails on different flight levels. Fig. 3(a) shows the pure cost-optimal trajectories (i.e., EI = 0.0). It can be seen that contrail-sensitive regions are crossed by aircraft. Whereas, as can be observed in Fig. 3(b), these regions are mostly avoided with the climate-optimal routing option, considering EI = 1.0. For the flight levels with no persistent contrails formation, such as FL280 and FL300, both routing strategies result almost in similar trajectories. The effects of increasing EI on ATR and simple operating cost are shown in Fig. 4a, 4b, respectively. As can be seen, higher EIs mitigate the climate impact with a slight increase in the cost. The errorbars in Fig. 4 show the ranges of uncertainty (standard deviation) due to the ensemble forecast. The Pareto-frontier, showing the trade-off between climate impact mitigation potential and relative increase in cost, is given in Fig. 4d. It can be concluded from Fig. 4d that there is a potential to reduce the climate impact by 28% at the expense of accepting 3% increase in cost.

5.2. Conflict assessment

To see how the adoption of climate-optimized routes affects the complexity of the considered network scenario, the number of conflicts is calculated using the approach presented in Section 4.1. A 4D grid is generated to evaluate the conflicts. The size of each cell is considered as $0.1° \times 0.1° \times 1000 ft \times 1s$ that is small enough in which no conflict is missed. We define a probability threshold (P_τ = 0.5 in this study) to differentiate between low and high probable conflicts. The conflicts with a probability less than 0.5 are labeled as low probability conflicts and vice versa for high probability ones. The number of conflicts for the considered eight EIs are provided in Fig. 4c, showing that climate impact reduction is achieved at the cost of increasing separation violation. Therefore, in addition to the cost, the increase in the number of conflicts is another challenge that arises with considering climate impact. To depict this fact, the geographical locations of conflicts for different routing options are plotted in Fig. 5. From Fig. 5, it can be concluded that the climate non-sensitive regions with less or no contrails climate impact become more congested with increasing EI. This is because the aircraft tend to fly in these areas to mitigate climate impact, resulting in loss of standard separation between aircraft. Therefore, there exists a trade-off between mitigating the climate impact and the number of conflicts. From Fig. 4d, one can conclude that the reduction of climate impact by 28% is achieved at the expense 65% increase in the number of conflicts (for EI = 1.0). It is worth mentioning that the range of uncertainty in the obtained cost (Fig. 4b) is neglectable. Moreover, most of the conflicts are high probable ones. One justification for such a low impact of uncertainty is the usage of reanalysis data. For weather forecast data, the ranges of uncertainty for the same scenario are expected to be higher.

---

[2] https://cds.climate.copernicus.eu/
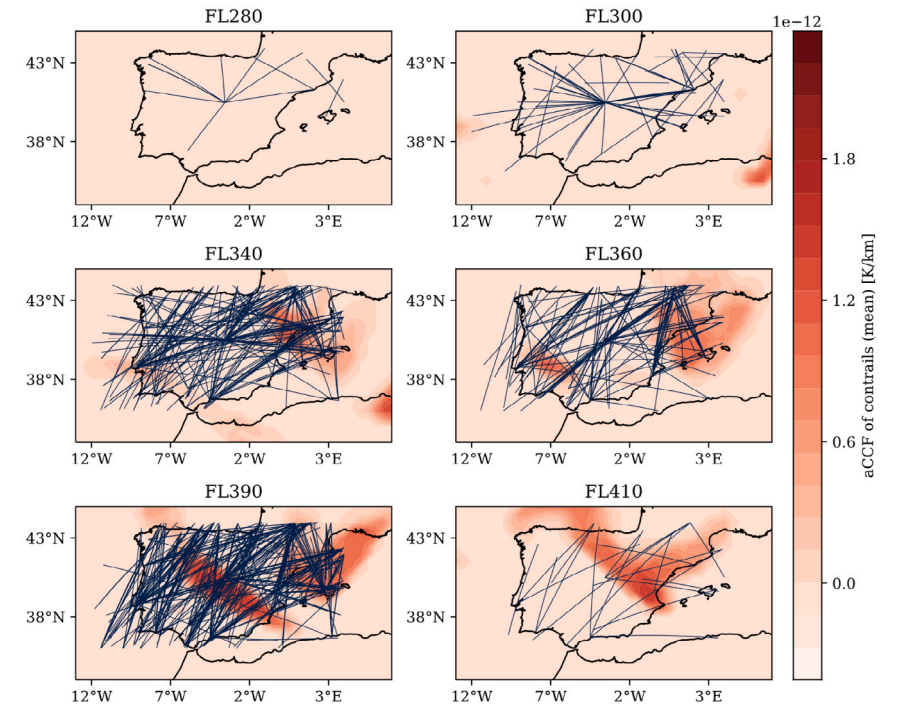
(a) cost-optimal routing option (EI = 0.0)
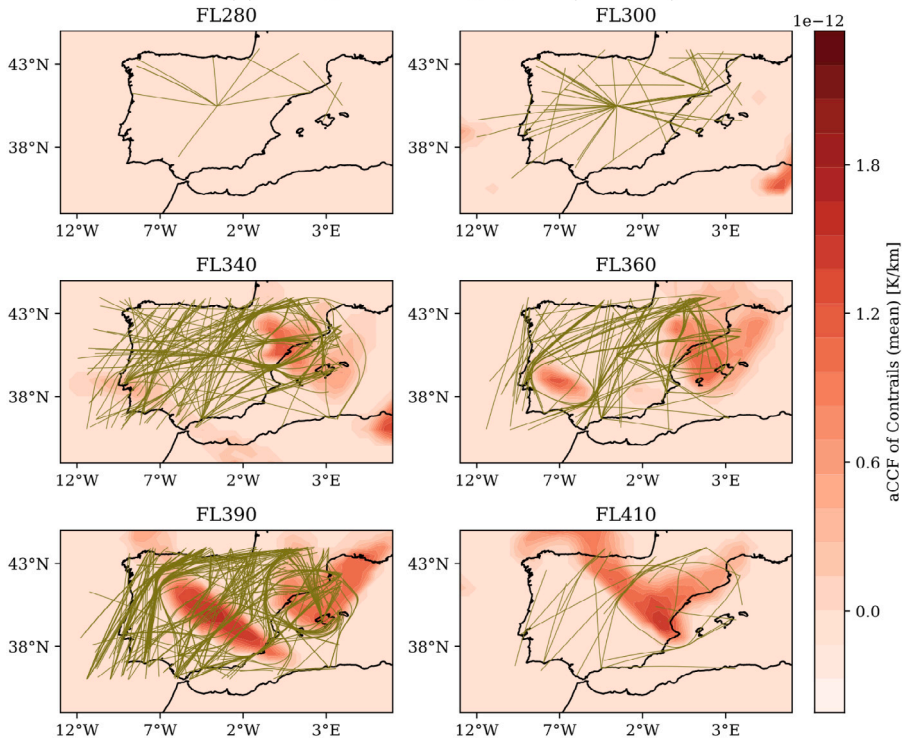
(b) climate-optimal routing option (EI = 1.0)

Fig. 3. Lateral paths depicted with the contrail-sensitive regions (aCCF of contrails) as colormaps for different flight levels.
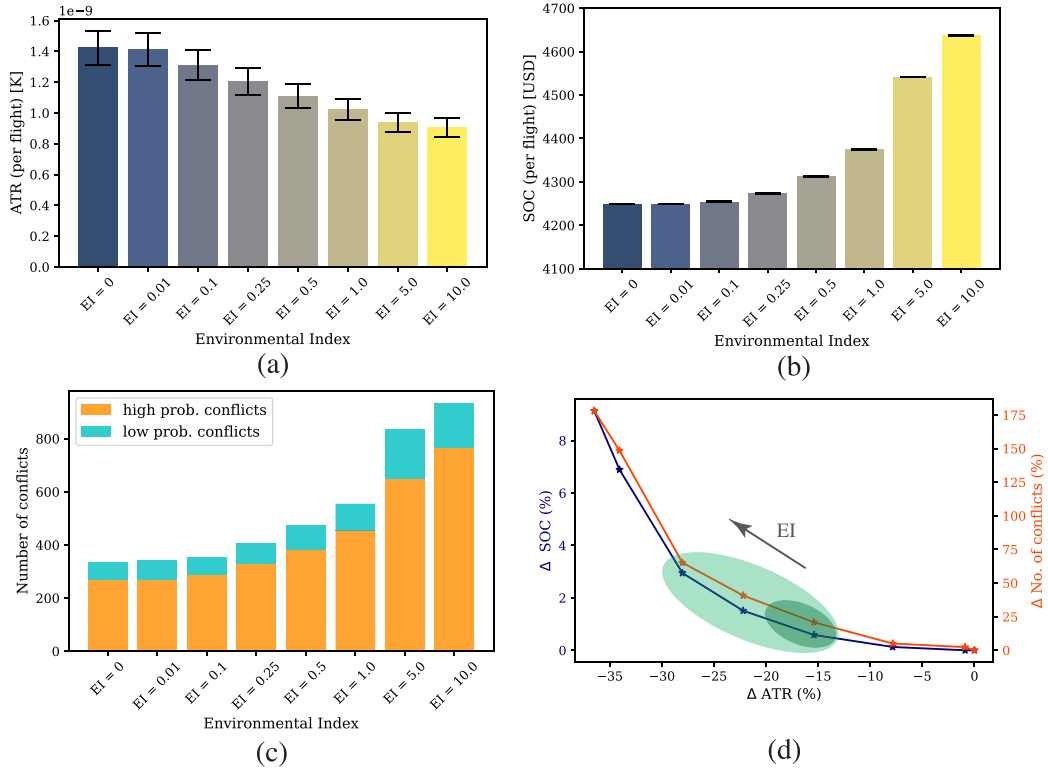
Fig. 4. The obtained performances for different EIs. SOC and ATR have been divided by the number of flights.

5.3. Conflict resolution

As was shown, the mitigation of climate impact is achieved at the expense of a significant increase in the number of conflicts for higher EIs, which may not be resolvable at the tactical level. Therefore, to strategically resolve the encountered conflicts, we employ the resolution algorithm presented in Section 4.2. To this end, four sets of optimized trajectories associated with different EIs (i.e., EI = 0.0, 1.0, 5.0, 10.0) are selected for the resolution process. For each set of trajectories, the proposed SA Algorithm 1 is implemented in Python for four different weighing coefficients β's (i.e., $\beta = 0.0, 0.1, 0.5, 1.0$) considering $K = 200$. In this study, we assign $P_\tau = 0.5$ for the probability threshold; thus, only the high probable conflicts are incorporated in the cost function to be resolved. Notice that at each iteration within the resolution algorithm, after modifying the speed of aircraft in conflict, the total number of conflicts between all aircraft is re-evaluated to consider the domino effect of de-conflicting one pair of aircraft on the others. The performance of the proposed resolution strategy in terms of climate impact, cost, and the number of conflicts are depicted in Fig. 6 for different EIs and β's. As can be seen in Fig. 6, for all sets of trajectories corresponding to different EIs, by increasing β, the number of high probability conflicts is reduced by a slight increase in cost and climate impact. The trade-off between reducing conflicts and relative increases in cost and climate impact is depicted in Fig. 7 for different sets of optimized trajectories. From Fig. 7, it can be concluded that the reduction of conflicts is achieved by accepting a very small increase in cost and climate impact. In all cases, by accepting less than 0.5% increase in cost and climate impact, the conflicts are reduced at least by 20%. It is worth mentioning that by increasing EI, the potential to resolve conflicts is reduced. Finally, the trade-off between reducing the number of conflicts and deviation from optimal speeds (obtained from trajectory optimization) is depicted in Fig. 8 by means of Pareto frontiers. The results indicate that the reduction of conflicts results in an increase in deviation from climate-optimal speed.

A brief summary of the performance of the proposed resolution algorithm is presented in Table 1. An observation from the number of modified aircraft trajectories implies that in almost all scenarios, less than 10% of aircraft trajectories are modified. Moreover, the number of seeded-up aircraft is almost similar to the slowed-down ones. Since the focus of resolution is on reducing high probable conflicts (due to the selection of P_τ), the number of low probable conflicts is increased in all cases.

5.4. Discussion on the implementation

The case study performed in this work raises an important question about the incentives for stakeholders and the required steps for implementing such a new routing strategy, i.e., climate-optimal flight plans. This is because the dependency of aviation-induced
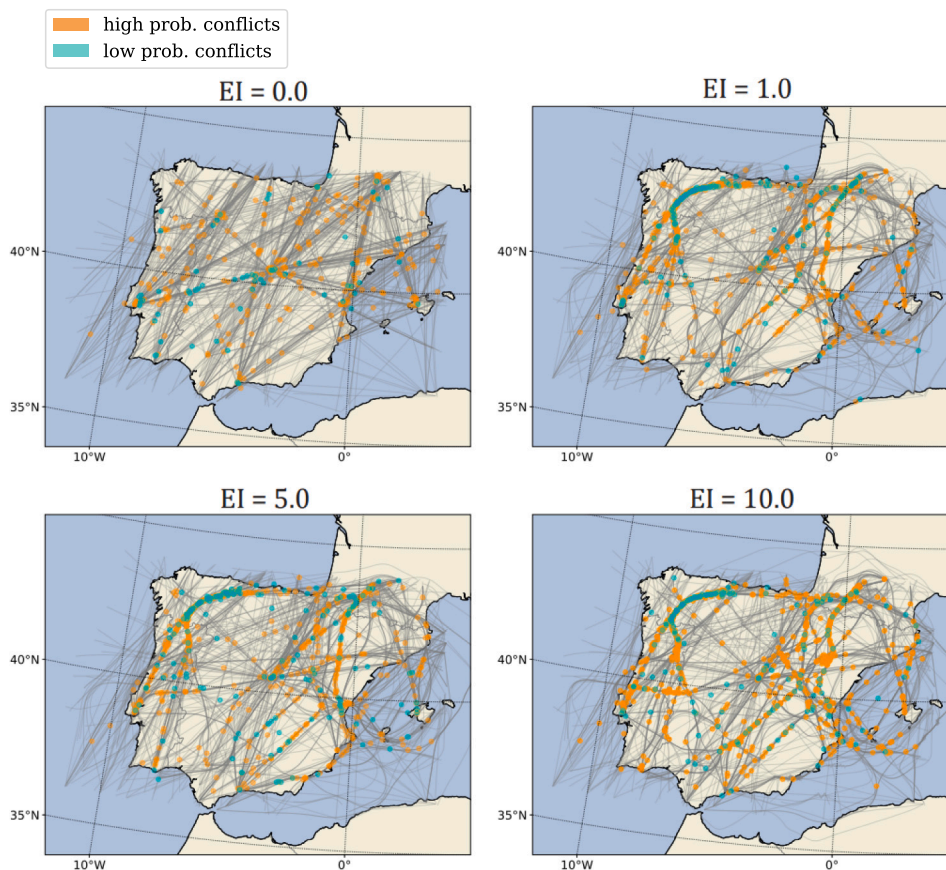
Fig. 5. Lateral paths with the location of high and low probability conflicts for different EIs.

climate effects on the meteorological conditions will lead to changes in traffic patterns, normally resulting in higher operating costs and also increased workload, complexity, and the number of conflicts. In this study, we quantified extra costs in a simplified manner (using simple operating costs) and also explored the possibility of reducing the number of conflicts with a resolution strategy. In the following, we will discuss some required steps toward implementing climate-optimal trajectories from a higher-level perspective:

First, a "MET-service" enabler is needed. The integration of climate information into the meteorological information channels is a must. In this sense, CLIMaCCF library (Dietmüller et al., 2022)[3] is a step forward in that direction. Nevertheless, uncertainties are still prevalent, indicating the need to conduct fundamental research to better understand, quantify, and eventually reduce these uncertainties. This will enhance the reliability of the information.

Once the climate information is embedded as part of the meteorological service, different stakeholders could use it. The possibilities are twofold:

On the one hand, flight dispatchers could incorporate into their software tools to calculate climate-optimized flight plans. However, this will come at a cost. Who is paying that extra cost? That is the question. We believe that the development of key performance indicators to quantify the cost (from an airline perspective) of flying in a climate-friendly manner is needed (Simorgh et al., 2023). This is a pre-condition for the development of market-based mechanisms to incentivize airlines/dispatchers to follow such climate-friendly flight plans. Under the current regulations, there is no incentive to fly non-CO_2 climate-optimal trajectories. However, the emission of CO_2 has been included in the planned market-based instruments such as EU ETS, and during 2013–2020, it has led to a total reduction in aviation net CO_2 emissions of 159 Million tonnes.[4] Such a strategy is currently under exploration for the aviation non-CO_2 climate effects. One alternative that has been suggested is to use the concept of equivalent CO_2 emissions (Niklaß et al., 2019). Based on this approach, the non-CO_2 emissions (or their climate effects) are converted to the equivalent CO_2 emission. Then, the environmental cost of CO_2 emission (e.g., from ETS) is applied to the non-CO_2 emissions. Another approach is based on the definition of climate-charged airspace (Niklaß et al., 2021). Within this concept, highly climate-sensitive areas are identified

---

[3] https://github.com/dlr-pa/climaccf

[4] https://www.eurocontrol.int/publication/european-aviation-environmental-report-2022
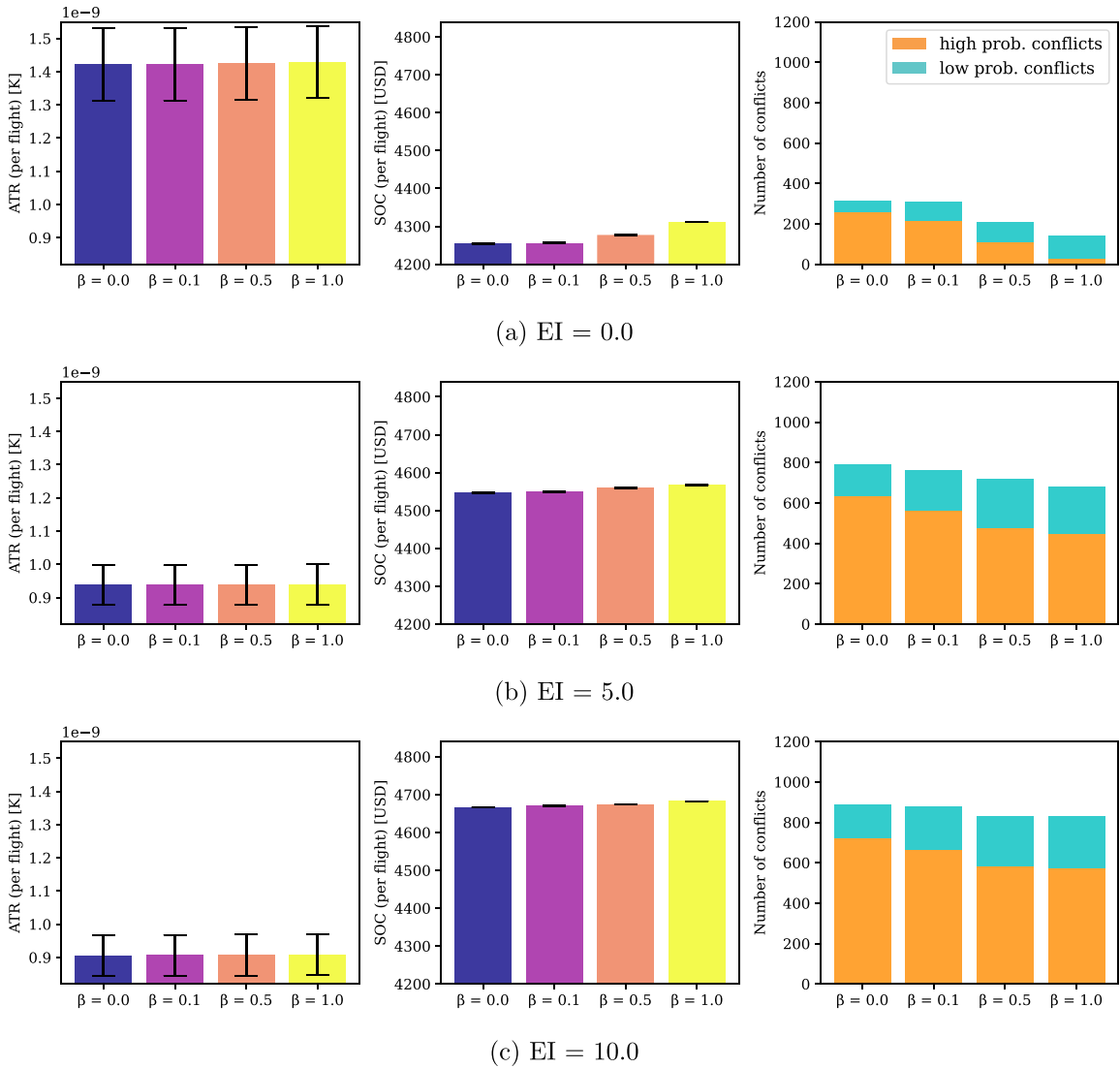
Fig. 6. The obtained results from the resolution method for different routing options (i.e., different EIs). For each routing option, the effects of increasing β (i.e., the weighing parameter in the cost function Eq. (16)) on the number of conflicts, simple operating cost, and climate impact are depicted. In all cases, the number of high-probability conflicts is reduced by a slight increase in cost and climate impact.

first. Then, taxes are considered for aircraft flying in these areas (Simorgh and Soler, 2022). CLIMaCCF library can be employed to provide such information on climate hotspots. All in all, the development of a market-based mechanism for aviation-induced climate effects can provide the possibility to compensate for the extra costs (associated with adopting climate-optimized flight plans) or even result in identifying win-win situations, in which both climate impact and operational costs get mitigated by flying climate-friendly routes.

On the other hand, the Network Manager and/or the Air Navigation Service Provider could integrate the climate impact (e.g., via CLIMaCCF) in their operational demand and capacity balancing tools. One possible approach would be the definition of ECHO Areas, which, in turn, would lead to traffic regulations (e.g., level capping). Nevertheless, this would also require the development of key performance indicators to quantify the cost (from a network perspective), e.g., in terms of complexity, safety, and capacity.

6. Conclusion & future works

This paper studied the impact of climate-aware flight planning on air traffic by assessing the number of potential conflicts. In our studied scenario, a set of 1005 flights were optimized for different objectives ranging from cost-optimal to climate-optimal routing options. The climate impacts were estimated employing algorithmic climate change functions. The uncertainty in the atmospheric variables was quantified employing ensemble weather forecasts and reflected on flight time, fuel consumption, and climate impact
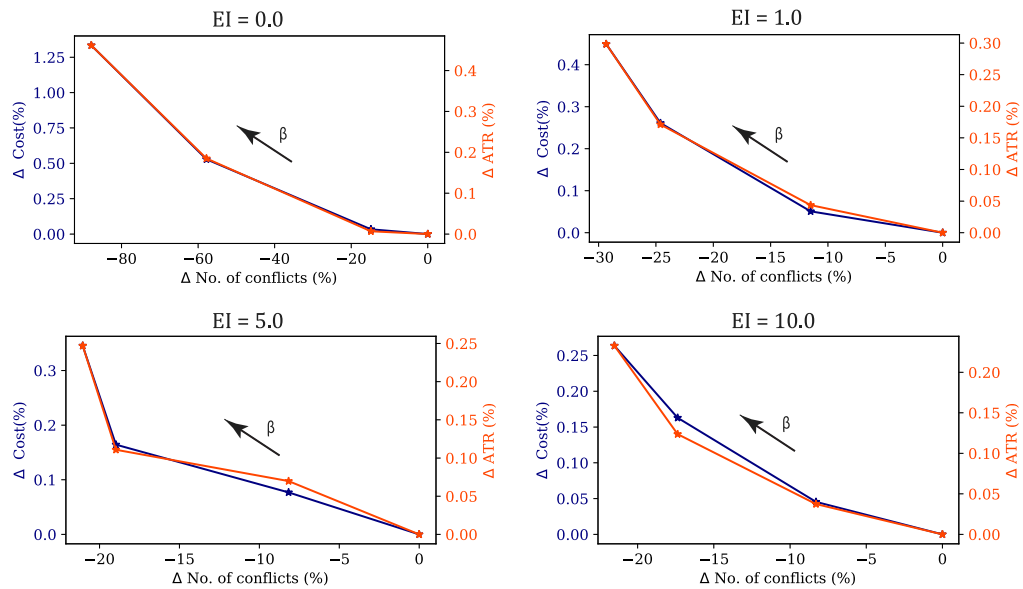
Fig. 7. Pareto-frontiers obtained by employing the proposed probabilistic resolution method for different sets of optimized trajectories (i.e., different EIs). The Pareto-frontiers show the trade-off between decreasing the number of high-probability conflicts and relative increases in cost and climate impact obtained using different β's.
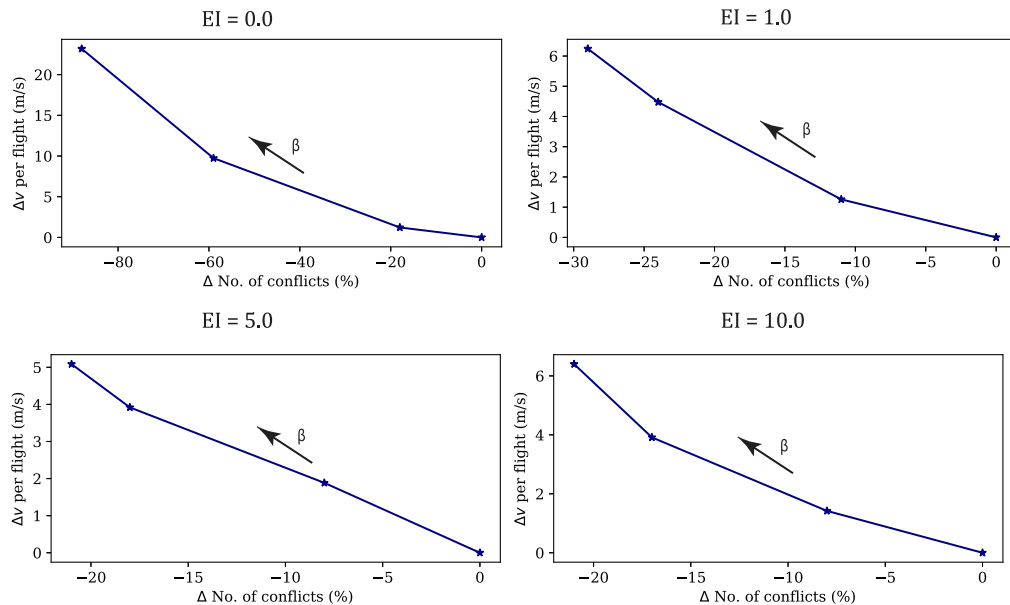

Fig. 8. Pareto-frontiers obtained by employing the proposed probabilistic resolution method for different sets of optimized trajectories (i.e., different EIs). The Pareto-frontiers show the trade-off between decreasing the number of high-probability conflicts and increase in deviations of speeds from the optimized ones obtained using different β's.

using ensemble trajectory prediction. The effects of adopting climate-optimized routes at the considered macro-scale scenario were then assessed in terms of operational cost and the number of conflicts. Pareto-frontiers were provided to study the existing trade-offs between climate impacts, cost, and the number of conflicts. We concluded that the number of conflicts increases quickly as we employ trajectories with lower climate impact. For example, in our case study, an overall 28% reduction in climate impact increased the number of conflicts by 65%, while a 7% more reduction in climate impact was achieved at the expense of a 110% additional increase in conflicts, which must be crucially taken into consideration. In this respect, we performed a strategic resolution using the SA algorithm to see how many conflicts can be reduced with only speed modifications and different weights penalizing deviation from climate-optimal trajectories. It was reported that by accepting less than 0.5% increase in cost and climate impact, at least

Table 1

A summary of the obtained results from the proposed resolution method for different sets of climate-optimal trajectories (i.e., different EIs). The effects of resolving high-probability conflicts for different values of β's, on the climate impact, cost, and the number of modified aircraft trajectories are reported.

Environmental Index	Performance	$\beta = 0.0$	$\beta = 0.1$	$\beta = 0.5$	$\beta = 1.0$
EI = 0.0	**ATR [K]**	$14.224e^{-8}$	$14.225e^{-8}$	$14.250e^{-8}$	$14.290e^{-8}$
	(*relative increase w.r.t. non-resolved trjs. [%]*)	(0%)	(0.006%)	(0.184%)	(0.461%)
	SOC [tUSD]	4.254	4.256	4.277	4.311
	(*relative increase w.r.t. non-resolved trjs. [%]*)	(0%)	(0.033%)	(0.528%)	(1.333%)
	High prob. conflicts	266	218	108	31
	(*relative decrease w.r.t. non-resolved trjs. [%]*)	(0%)	(18%)	(59%)	(88%)
	Low prob. conflicts	65	92	99	110
	Average speed variation [m/s]	0	1.223	9.738	23.177
	Number of speeded up aircraft	0	29	70	132
	Number of slowed down aircraft	0	28	81	150
EI = 5.0	**ATR [K]**	$9.362e^{-8}$	$9.375e^{-8}$	$9.381e^{-8}$	$9.393e^{-8}$
	(*relative increase w.r.t. non-resolved trjs. [%]*)	(0%)	(0.043%)	(0.171%)	(0.298%)
	SOC [tUSD]	4.547	4.549	4.558	4.567
	(*relative increase w.r.t. non-resolved trjs. [%]*)	(0%)	(0.050%)	(0.261%)	(0.449%)
	High prob. conflicts	634	561	478	448
	(*relative decrease w.r.t. non-resolved trjs. [%]*)	(0%)	(11%)	(24%)	(29%)
	Low prob. conflicts	157	197	221	235
	Average speed variation [m/s]	0	1.257	4.476	6.241
	Number of speeded up aircraft	0	20	33	31
	Number of slowed down aircraft	0	24	37	49
EI = 10.0	**ATR [K]**	$9.059e^{-8}$	$9.065e^{-8}$	$9.069e^{-8}$	$9.081e^{-8}$
	(*relative increase w.r.t. non-resolved trjs. [%]*)	(0%)	(0.069%)	(0.110%)	(0.247%)
	SOC [tUSD]	4.666	4.669	4.674	4.682
	(*relative increase w.r.t. non-resolved trjs. [%]*)	(0%)	(0.076%)	(0.164%)	(0.345%)
	High prob. conflicts	722	663	585	564
	(*relative decrease w.r.t. non-resolved trjs. [%]*)	(0%)	(8%)	(18%)	(21%)
	Low prob. conflicts	167	215	246	259
	Average speed variation [m/s]	0	1.884	3.919	5.085
	Number of speeded up aircraft	0	31	35	23
	Number of slowed down aircraft	0	17	35	36

20% of conflicts could be resolved for all routing options. In addition, it was shown that the potential to reduce conflicts using speed change as the only decision variable is decreased by moving toward trajectories with lower climate impacts. For instance, for the cost-optimal routing option, 80% of the conflicts are resolvable, whereas, for the trajectories with less climate impact, the reduction is limited to 25%. Including other decision variables in the resolution, such as departure time, lateral path, and altitude, are alternatives that may increase this potentiality by resolving encountered conflicts in a more efficient manner (having more degrees of freedom).

Future works

A limitation of the analysis performed in the current study is the usage of lateral-only optimization. Therefore, follow-up work will be performed to consider the full 4D trajectory optimization problem, where the flight level can be changed in addition to the lateral path. Instead of the two-step procedure (i.e., deterministic optimization and ensemble trajectory prediction) to determine climate-optimized trajectories, we aim to directly solve the robust trajectory optimization problem, considering all ensemble members. In addition to the free-routing context, the study will also be extended to the optimization and complexity assessment within the currently structured airspace.

Given our conclusion regarding the number of conflicts and the added complexity, and also the reduction of potential to decrease the number of conflicts in the resolution process for trajectories with lower climate impacts, we propose follow-up studies exploring traffic planning strategies based on other decision variables such as change of lateral path, altitude profile and departure time to keep the airspace manageable. For the next steps, we plan to perform the resolution considering other indicators, including capacity-demand balancing, different complexity metrics, and congestion, as objectives to be optimized with minimum modifications to the climate-optimized trajectories.

References

Allignol, C., Barnier, N., Durand, N., Gondran, A., Wang, R., 2017. Large scale 3D en-route conflict resolution. In: ATM Seminar, 12th USA/Europe Air Traffic Management R&D Seminar.

Andrei, N., 2017. A SQP algorithm for large-scale constrained optimization: SNOPT. In: Continuous Nonlinear Optimization for Engineering Applications in GAMS Technology. Springer, pp. 317–330.

Bauer, P., Thorpe, A., Brunet, G., 2015. The quiet revolution of numerical weather prediction. Nature 525 (7567), 47–55. http://dx.doi.org/10.1038/nature14956.

Betts, J.T., 2010. Practical methods for optimal control and estimation using nonlinear programming, second ed. In: Advances in Design and Control, SIAM.

Biegler, L.T., Zavala, V.M., 2009. Large-scale nonlinear programming using IPOPT: An integrating framework for enterprise-wide dynamic optimization. Comput. Chem. Eng. 33 (3), 575–582.

Courchelle, V., Soler, M., González-Arribas, D., Delahaye, D., 2019. A simulated annealing approach to 3D strategic aircraft deconfliction based on en-route speed changes under wind and temperature uncertainties. Transp. Res. C 103, 194–210.

Dietmüller, S., Matthes, S., Dahlmann, K., Yamashita, H., Simorgh, A., Soler, M., Linke, F., Lührs, B., Meuser, M.M., Weder, C., Grewe, V., Yin, F., Castino, F., 2022. A python library for computing individual and merged non-CO_2 algorithmic climate change functions: CLIMaCCF V1.0. Geosci. Model Dev. Discuss. 2022, 1–33. http://dx.doi.org/10.5194/gmd-2022-203, URL https://gmd.copernicus.org/preprints/gmd-2022-203/.

Dowsland, K.A., Thompson, J., 2012. Simulated annealing. Handb. Nat. Comput. 1623–1655.

DuBois, D., Paynter, G.C., 2006. "Fuel flow method2" for estimating aircraft emissions. SAE Trans. 1–14.

Gallo, E., Navarro, F., Nuic, A., Iagaru, M., 2006. Advanced aircraft performance modeling for ATM: Bada 4.0 results. In: 2006 Ieee/Aiaa 25TH Digital Avionics Systems Conference. IEEE, pp. 1–12. http://dx.doi.org/10.1109/dasc.2006.313660.

González Arribas, D., Andrés-Enderiz, E., Soler, M., Jardines, A., García-Heras, J., 2020.Probabilistic 4D Flight Planning in Structured Airspaces through Parallelized Simulation on GPUs.In: 9th International Conference for Research in Air Transportation, ICRAT.

González-Arribas, D., Soler, M., Sanjurjo-Rivo, M., García-Heras, J., Sacher, D., Gelhardt, U., Lang, J., Hauf, T., Simarro, J., 2017. Robust optimal trajectory planning under uncertain winds and convective risk. In: ENRI International Workshop on ATM/CNS. Springer, pp. 82–103.

Hastings, E.J., Mesit, J., Guha, R.K., 2005. Optimization of large-scale, real-time simulations by spatial hashing. In: Proc. 2005 Summer Computer Simulation Conference, Vol. 37, no. 4. pp. 9–17.

Hernández Romero, E., 2020. Probabilistic aircraft conflict detection and resolution under the effects of weather uncertainty.

Hilburn, B., 2004. Cognitive complexity in air traffic control: A literature review. EEC Note 4 (04), 1–80.

Jakšić, Z., Janić, M., 2020. Modeling resilience of the ATC (air traffic control) sectors. J. Air Transp. Manag. 89, 101891.

Lee, D.S., Fahey, D., Skowron, A., Allen, M., Burkhardt, U., Chen, Q., Doherty, S., Freeman, S., Forster, P., Fuglestvedt, J., et al., 2021. The contribution of global aviation to anthropogenic climate forcing for 2000 to 2018. Atmos. Environ. 244, 117834.

Matthes, S., Grewe, V., Dahlmann, K., Frömming, C., Irvine, E., Lim, L., Linke, F., Lührs, B., Owen, B., Shine, K., et al., 2017. A concept for multi-criteria environmental assessment of aircraft trajectories. Aerospace 4 (3), 42.

Matthes, S., Lührs, B., Dahlmann, K., Grewe, V., Linke, F., Yin, F., Klingaman, E., Shine, K.P., 2020. Climate-optimized trajectories and robust mitigation potential: Flying ATM4E. Aerospace 7 (11), 156.

Niklaß, M., Dahlmann, K., Grewe, V., Maertens, S., Plohr, M., Scheelhaase, J., Schwieger, J., Brodmann, U., Kurzböck, C., Schweizer, N., et al., 2019. Integration of Non-CO2 Effects of Aviation in the EU ETS and under CORSIA. Umweltbundesamt.

Niklaß, M., Grewe, V., Gollnick, V., Dahlmann, K., 2021. Concept of climate-charged airspaces: A potential policy instrument for internalizing aviation's climate impact of non-CO_2 effects. Clim. Policy 21 (8), 1066–1085.

Pejovic, T., Netjasov, F., Crnogorac, D., 2020. Relationship between air traffic demand, safety and complexity in high-density airspace in Europe. In: Risk Assessment in Air Traffic Management. IntechOpen.

Pelegrín, M., d'Ambrosio, C., 2022. Aircraft deconfliction via mathematical programming: Review and insights. Transp. Sci. 56 (1), 118–140.

Prandini, M., Piroddi, L., Puechmorel, S., Brázdilová, S.L., 2011. Toward air traffic complexity assessment in new generation air traffic management systems. IEEE Trans. Intell. Transp. Syst. 12 (3), 809–818.

Simorgh, A., Soler, M., 2022. Non-CO2 market-based incentives towards robust climate optimal aircraft trajectories. In: Proceedings of International Workshop on ATM/CNS, Vol. 1. pp. 156–163. http://dx.doi.org/10.57358/iwac.1.0_156.

Simorgh, A., Soler, M., González-Arribas, D., Linke, F., Lührs, B., Meuser, M.M., Dietmüller, S., Matthes, S., Yamashita, H., Yin, F., Castino, F., Grewe, V., Baumann, S., 2023. Robust 4D climate optimal flight planning in structured airspace using parallelized simulation on GPUs: ROOST V1.0. EGUsphere 1–39. http://dx.doi.org/10.5194/egusphere-2022-1013, URL https://egusphere.copernicus.org/preprints/egusphere-2022-1013/.

Simorgh, A., Soler, M., González-Arribas, D., Matthes, S., Grewe, V., Dietmüller, S., Baumann, S., Yamashita, H., Yin, F., Castino, F., Linke, F., Lührs, B., Meuser, M.M., 2022. A comprehensive survey on climate optimal aircraft trajectory planning. Aerospace 9 (3), http://dx.doi.org/10.3390/aerospace9030146, URL https://www.mdpi.com/2226-4310/9/3/146.

Socha, V., Hanáková, L., Valenta, V., Socha, L., Ábela, R., Kušmírek, S., Pilmannová, T., Tecl, J., 2020. Workload assessment of air traffic controllers. Transp. Res. procedia 51, 243–251.

Tran, N.P., Pham, D.-T., Goh, S.K., Alam, S., Duong, V., 2019. An intelligent interactive conflict solver incorporating air traffic controllers' preferences using reinforcement learning. In: 2019 Integrated Communications, Navigation and Surveillance Conference. ICNS, IEEE, pp. 1–8.

van Manen, J., Grewe, V., 2019. Algorithmic climate change functions for the use in eco-efficient flight planning. Transp. Res. Part D: Transp. Environ 67, 388–405.

WMO, 2012. Guidelines on ensemble prediction systems and forecasting, Vol. 1091. World Meteorological Organization Weather Climate and Water.

Yamashita, H., Yin, F., Grewe, V., Jöckel, P., Matthes, S., Kern, B., Dahlmann, K., Frömming, C., 2020. Newly developed aircraft routing options for air traffic simulation in the chemistry–climate model EMAC 2.53: AirTraf 2.0. Geosci. Model Dev. 13 (10), 4869–4890.

Yamashita, H., Yin, F., Grewe, V., Jöckel, P., Matthes, S., Kern, B., Dahlmann, K., Frömming, C., 2021. Analysis of aircraft routing strategies for north atlantic flights by using AirTraf 2.0. Aerospace 8 (2), 33.